The International Journal of Advanced Manufacturing Technology (2022) 122:1339–1351
https://doi.org/10.1007/s00170-022-09992-6

ORIGINAL ARTICLE

Strategies for adjusting process parameters in CAE simulation to meet real injection molding condition of screw positions and cavity pressure curves

Bo-Wei Wang[1] · Shih-Chih Nian[2] · Ming-Shyan Huang[1]

Received: 2 June 2022 / Accepted: 16 August 2022 / Published online: 20 August 2022

Abstract
Numerical simulations of polymer melt flow behavior in mold cavities help optimize process parameters. However, mathematical models, processing conditions, material property settings, and machine aging can cause simulations to differ from experimental results. The accuracy of simulations can indicate injection mold quality, which is used to determine the optimal process parameters. However, the optimal process parameters for simulations are very different from the real situation and cannot be directly applied in practice. Therefore, the simulation setup in the manufacturing process requires additional molding trials, resulting in time and cost consumption. This study used high-precision injection molding machines, material property settings, mold dimensions, and mold temperatures to assess the difference in pressure curves between simulations and real molding. This study also developed a method for adjusting the injection molding process parameters of a simulation to decrease the difference in pressure and screw position curves between the simulation and real molding, thus quantitatively improving the quality prediction capacity of simulations. The results contribute to the research on directly applying the injection molding process parameters of a simulation to real molding to achieve smart manufacturing.

Keywords Cavity pressure · Injection molding · Smart manufacturing · Mold flow simulation

1 Introduction

With the development of Industry 4.0, the digitalization of the manufacturing industry has become a topic of global concern, especially for the injection molding industry, which requires low costs, automation, high production efficiency, competitiveness, and safe human–machine collaboration to achieve smart manufacturing. The core of smart manufacturing is digital (information) technology that automatically collects and analyzes data during the product manufacturing process. Given the continuous accumulation of manufacturing data, the construction of cyber-physical systems with artificial intelligence technology can facilitate sensible decision-making and optimize processes. In the field of injection molding, although powerful mold flow simulation software has assisted in optimizing product design, mold design, and part quality evaluation, simulations for determining the optimal process parameters require high accuracy before the parameters can be applied to molding. Although applying sensing technology to tasks such as identifying cavity pressure curves to determine the physical flow behavior of polymer melts can help optimize process parameters during molding, the cost and feasibility of sensors limit their use, thus necessitating simulations. However, because of a lack of accurate information regarding the machines, molds, processed resins, auxiliary devices, environmental noise, and human factors that affect the quality of molded parts, simulated molding differs considerably from real molding. This may be due to differences in injection speed response time between simulations and real scenarios. In particular, the heat transfer

✉ Ming-Shyan Huang
mshuang@nkust.edu.tw

Bo-Wei Wang
f108102102@nkust.edu.tw

Shih-Chih Nian
lawren@ntct.edu.tw

[1] Department of Mechatronics Engineering, Yanchao Dist, National Kaohsiung University of Science and Technology, 1 University Road, Kaohsiung City 824, Taiwan

[2] Department of Power Mechanical Engineering, National Taitung College, No. 911 Zhengqi North Road, Taitung City 950, Taiwan

coefficient, viscosity, and compressibility of the processed resins under various pressure and temperature conditions may be the main variables for discrepancies between the molding and simulation results. Other sources of error, such as check ring leakage, can also cause discrepancies. Mold rigidity can reduce pressure attenuation in the holding stage considerably, especially for thin-walled molding, in which the pressure curve controls the residual stress acting on the polymer melt. In addition, in the Williams–Landel–Ferry model, which is widely used in injection molding simulation software because of its simplicity, a considerable difference is evident between the pressure predicted by CAE molding simulations and the pressure observed by real molding operators, resulting in the selection of inappropriate machines for injection molding or erroneous mold design.

The injection molding process parameters that most strongly affect molding quality are melt temperature, cooling temperature, injection speed, the velocity-to-pressure (V/P) switchover point, holding pressure and time, clamping force, and back pressure. These process parameters can be systematically optimized using sensor technology to determine the cavity pressure, screw position, and melt temperature of a polymer melt in the injection molding process. To consistently produce high-quality parts, the quality of injection molding must be monitored in addition to the quality of the process parameters. Cavity pressure is an indicator of molding quality. However, sensing is costly and requires installation space, and simulations must be accurate when the pressure curve is applied to quality control. Therefore, eliminating the difference between the results of simulated and real molding is essential and represents the purpose of this research.

2 Literature review

Injection molding is a pressure-driven process. Polymer melts require pressure to overcome resistance when flowing through nozzles, sprues, runners, and gates and entering cavities. Therefore, the system pressure determines the quality of injection molding. The cavity pressure curve can indicate the quality of injection-molded parts (e.g., short shot and flash), and by examining the slope of the cooling phase, the shrinkage rate of parts can be determined [1]. The cavity pressure curve is usually used to monitor the quality of repeated injections. However, repeated injections with the same machine parameter settings may produce different cavity pressure curves at the end of the flow. This indicates that high-precision injection molding machines do not guarantee consistent injection molding quality.

Various sensing technology methods can be used to determine the flow behavior of polymer melts in a mold. Therefore, the injection molding process no longer relies on engineers' experience to determine the process parameter settings that ensure high quality and yield. Instead, the process requires sensor data provided by an injection molding machine and several sensors installed in the mold or machine. Sensors can be divided into in-mold sensors, nozzle sensors, and tie-bar sensors depending on their installation position. In-mold sensors include pressure and temperature sensors, which are used to determine the flow behavior of polymer melts in sprue–runner–gate and cavity systems [2–7]. Nozzle sensors are used to identify changes in the viscosity of polymer melt as it flows from a barrel and passes through a nozzle, which helps to monitor the quality of plasticization before injection into the mold [8–12]. Tie-bar sensors include strain gauges and ultrasonic sensors. They are installed in the machine and are nondestructive to the mold, which is why they are also called "nondestructive sensors." Although they are not as sensitive a sensor as cavity pressure, they are useful in quality monitoring and control [13–20].

Beaumont [21] studied a Therma-flo method that accounts for the effect of part thickness and melt and mold temperature on polymer melt rheology and concluded that for certain thick parts and fast injection speeds, melt temperature can be balanced through adjustments to shear and thermodynamic heat. Hopmann and Zhuang [22] determined the injection pressures required for various filling time settings and identified an optimal injection speed that produces the least resistance during the filling process. The optimal injection speed also resulted in a minimal change in viscosity, helping to achieve consistent quality in mass production [23]. Karbasi [24] revealed that temperature affects pressure distribution, especially in the plasticizing phase and V/P switchover point. Nian et al. [25] used in-mold machine signals to set the ideal injection speed, injection speed segment, V/P switchover point, and holding conditions on the basis of screw position and cavity pressure. Similarly, Chang et al. [26] applied infrared temperature and cavity pressure sensors to detect melt temperature and pressure and adjusted the holding conditions to minimize part shrinkage on the basis of pressure–volume–temperature (pvT) theory.

With Industry 4.0, cyber-physical systems have become the primary method of intelligent injecting molding, in which mold flow simulation is crucial; eliminating the difference between the results of simulations and real scenarios is the main purpose. Simulation accuracy is limited when simplified mathematical models are employed and is also limited by material property settings, process parameter conditions, and machine performance and aging. Guerrier et al. [27] and Regi et al. [28] regarded the modeling of the machine nozzle and barrel as a hot runner system. The new model increased the consistency of filling times and filling patterns between simulations and real molding. The amount of polymer melt

compression in the filling phase must be considered in a simulation. Huang et al. [29, 30] indicated that a machine's response to the speed command affects the simulation of the filling phase. By calibrating the speed response, the simulation accuracy for speed and pressure can be increased. However, additional factors must be evaluated to further increase simulation accuracy [31].

This study developed a process parameter adjustment technology to eliminate the difference between the results of simulation and real molding. An in-mold machine molding trial method is proposed herein for determining the optimal process parameter settings on the basis of pressure and screw position curves. The process parameters for the simulation, namely, filling stroke, injection speed, and filling-to-packing V/P switchover point, are adjusted on the basis of the ideal pressure and screw position observed during real molding. The process is as follows:

1. Calibrating the full volumetric filling point: by adjusting the filling stroke of the screw position, consistency between the simulation and real molding can be achieved. Consistency in flow behavior helps to adjust the difference in pressure. This process involves complex compression of the polymer melt, which is often inaccurately predicted by simulations.
2. Calibrating the system pressure curve: the injection speed in the simulation is adjusted on the basis of the results of step 1. The system pressure reflects the history of the polymer melt in terms of the system pressure required to overcome resistance when flowing through nozzles, sprues, runners, gates, and cavities. With the history of the screw position, system pressure can be used to determine the change in viscosity and energy working on the polymer melt during the molding process.
3. Calibrating the cavity pressure curve: the V/P switchover point in the simulation is adjusted on the basis of the results of step 2 to ensure the simulated cavity pressure curve is consistent with that observed during real molding. Cavity pressure reflects the history of a polymer melt's behavior in the cavity during filling, holding, and cooling. The cavity pressure curve indicates injection molding quality and has been used to determine the optimal process parameter settings and predict the quality of injection-molded parts.
4. Quality comparison: the width reduction rate in the simulation after process parameter adjustment is compared with that observed during real molding.

To determine the feasibility of this method, this study examined injection-molded flat plates and compared the simulated pressure and screw position curves before and after calibration with those observed during real molding.

3 Methodology

3.1 In-mold and machine sensing-based molding trial method

The molding trial method based on in-mold machine sensing involves using the information regarding the pressure of the polymer melt in the cavity and the system pressure and screw position of the injection molding machine to identify the ideal process parameters. Screw position and pressure history during injection molding can be used to distinguish the filling, packing, V/P switchover, and cooling phases. The optimal process parameters can be quickly and accurately obtained by using the cavity pressure curve. In injection molding machine production, using the curve as the standard cavity pressure curve can reduce the time required for debugging and setting the process parameters.

The process comprises three steps:

1. Optimizing injection speed during the filling stage: during the filling phase, the injection molding machine performs speed control and employs an upper-limit pressure strategy for the injection screw, which pushes the polymer melt into the cavity. The optimal injection speed is determined on the basis of the minimum pressure drop between the near-gate area and the end of the filling area under various injection speed settings;
2. Optimizing the V/P switchover point: by observing the screw position and pressure history curve, early, late, and ideal timing for switching between the speed control of the injection screw and the pressure control during the mold filling and packing phases can be determined. With early timing, pressure decreases considerably then increases at the switching point. With late timing, pressure peaks. Ideal timing produces a stable pressure curve [25]; and
3. Optimizing the holding pressure and time during the holding phase: by observing the screw position and hold time, the minimum packing time sufficient to compensate for plastic shrinkage can be determined. Several holding conditions are used to determine the process parameters to produce high-quality parts. With the four pressure sensors installed along the filling path (A_1 to A_4) as an example, the steps for setting multistage holding pressure and time are as follows [32]:

    (a) Determine the effective holding time—the solidification time of the gate. After the gate is solidified, the melt no longer enters the cavity, and the pressure curve near the gate is no longer affected by the injection pressure outside the gate, allowing the effective holding time to be determined. The holding pressure is initially set to zero then changed to a

higher holding pressure (P_{pulse}); the pressure curve close to the gate can then be observed. The effective hold time ($t_{\Sigma,hold}$) represents the minimum holding time during which the pressure curve close to the gate is not affected by P_{pulse};

(b) Set the holding pressure time for each stage. Similar to (a), the holding pressure is initially set to zero and then increased (P_{pulse}). The holding pressure in the first stage of this case study was set to fully compensate for the volumetric shrinkage of the molded part in the area far from the gate. The first-stage holding time (t_{S_4}) in Fig. 1 represents the minimum holding time during which the pressure curve close to A_4 is not affected by P_{pulse}. The second-stage (t_{S_2}), third-stage (t_{S_3}), and fourth-stage holding times (t_{S_4}) are determined using A_3, A_2, and A_1, where $t_{S2} = t_{A_3} - t_{A_4}$, $t_{S3} = t_{A_2} - t_{A_3}$, and $t_{S4} = t_{\Sigma,hold} - t_{A_2}$; and

(c) Set the holding pressure for each stage. The first-stage holding pressure is the same as the single-stage holding pressure to ensure it compensates for the quality of the plastic parts at the far gate (A_4). The second-stage holding pressure is then reduced. At each induction position, the pressure curve close to the gate must be greater than the pressure curve at the far gate to prevent the melt from flowing back into the cavity; hence, the cavity pressure curve should follow $P_{A_1} > P_{A_2} > P_{A_3} > P_{A_4}$.

3.2 Process parameter adjustment in simulation

Because the cavity pressure and screw position curves are determined by factors such as injection speed, V/P switchover, and holding pressure, this study evaluated adjusting these factors to calibrate the simulated pressure curves. First, this study referred to the real system pressure history and adjusted the metering stroke and injection speed in the simulation to ensure consistency in peak pressure, the foremost position of the injection screw, and the V/P switchover timing between the simulation and real molding. This study also referred to the cavity pressure history and adjusted the V/P switchover point to increase consistency.

4 Experimental setup

Figure 2 presents a flat plate with a length of 200 mm, a width of 60 mm, and thicknesses of 1.5, 1, and 2 mm along the flow channel. The plate has a high ratio of flow length to thickness (more than 150). The middle of the plate has a rectangular hole. The diameter of the sprue of the injection mold is 3.5–6 mm, and the thickness of the fan gate is 2–1.5 mm. The cooling system consists of four linear channels with a diameter of 8 mm, and two channels each are used for the male and female mold plates. The processed polymer material was acrylonitrile butadiene styrene, which is an amorphous material (PA756, Chi-Mei Corporation, Taiwan). Figure 2 also displays the measurement position of the part width, where W1, W2, and W3 represent the injection molding quality of the 1.5-mm-thick area and W4 and W5 represent the quality of the 1- and 2-mm-thick areas, respectively. The width was measured with a three-coordinate measuring machine (CRYSTA-Apex S 7106, Mitutoyo Corporation, Japan). This study used a high-precision all-electric injection molding machine (S2000i100B, Fanuc Corporation, Japan) with a maximum clamping force of 1000 kN, a screw diameter of 28 mm, a maximum injection pressure of 240 MPa, and a maximum injection speed of 500 mm/s. The screw stroke was 95 mm. An oil-heating mold temperature

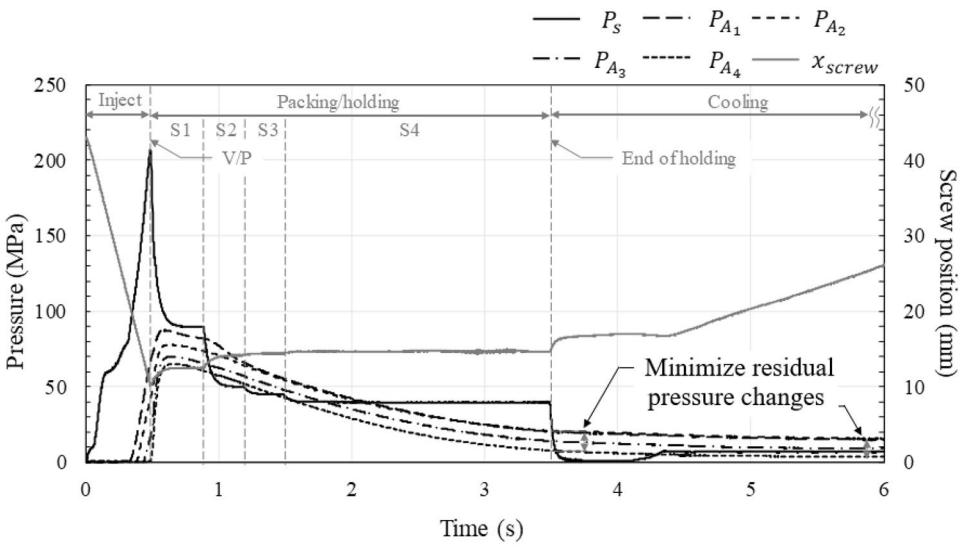

Fig. 1 Sensed pressure curves at positions A_1 to A_4 with appropriate V/P switchover point and multistage holding process at mold filling and holding stages [32]

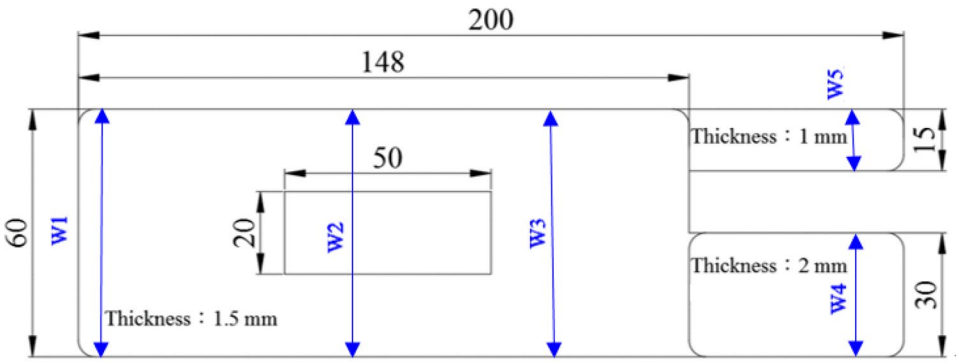

Fig. 2 Injection-molded part: geometric dimensions and measuring position for width

control device (YBMI-200–20, Taiwan Yann Bang Electrical Machinery Co., Ltd., Taiwan) was used for the experiment.

Figure 3 displays the positions of the eight pressure sensors installed in the injection mold. P1, P2, and P3 measure the pressure history at the bottom of the sprue and the front and back of the fan gate, respectively. P4 and P5 measure the pressure history when the 1.5-mm-thick area is filled. P6 and P8 measure the pressure history when the 1-mm-thick area is filled. P7 measures the pressure history when the 2-mm-thick area is filled. This study used two types of pressure sensors (SSB04KN10 × 08H and SSB16KN12 × 10H, Futaba Corporation, Japan). The first was used to measure the cavity pressure, and the second was used to measure the pressure in the sprue–runner–gate system. Figure 3 also displays the position of the three thermocouple sensors installed on the female mold plate (KEX-H-7/0.3 × 2, Championtech Technology Co., Ltd., Taiwan). T1, T2, and T3 were used to measure the mold temperature history. The pressure, screw position, and temperature signals were collected using a data acquisition card (USB-6343 DAQ, National Instruments Co., USA).

For the mold flow simulation, this study used Moldex3D 2020 Studio (R1OR version, CoreTech System Co., Ltd., Taiwan). This version provides a three-dimensional simulation of polymer melt compression in the barrel, allowing injection pressure to be accurately predicted [33]. This study used a model of a full mold base with a hybrid mesh for the mold flow simulation. The total number of mesh elements was approximately 10 million. Figure 4 displays the consistency between the simulation and real molding under various mold temperatures at T1, T2, and T3. When the mold temperature was 60 °C, the difference between the simulation and the real molding was less than 1 °C.

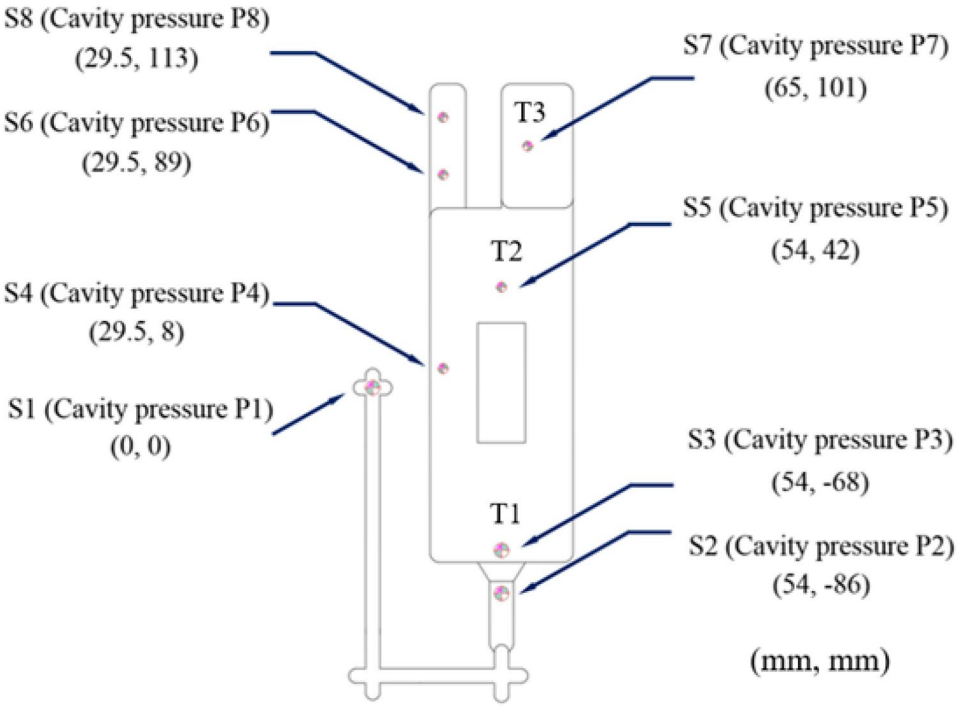

Fig. 3 Sensing position: pressure (P1 – P7) and temperature (T1 – T2)

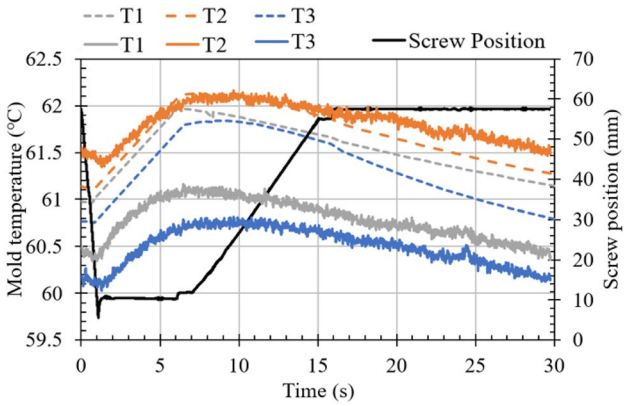

Fig. 4 Mold temperature curves (dashed line: simulation; solid line: real molding)

5 Results and discussion

5.1 Real molding

The real molding process followed the molding trial process based on in-mold machine sensing [25]. The first step was to determine the optimal injection speed on the basis of the minimal pressure drop along the filling path and to determine the injection speed segmentation that would ensure consistent melt-front speeds in various cross-sectional areas. Table 1 presents the process parameter settings in the real molding experiment. Figure 5a presents the system pressure drop under various injection speed settings. When the injection speed was 60 – 70 mm/s, the minimum pressure drop was observed along the flow path of P3 and P5. Therefore, the optimal speed was determined to be 70 mm/s, which allows for the lowest flow resistance. The simulation results are consistent with the real molding results (Fig. 5b).

To determine the appropriate V/P switchover point (usually 95 – 98% cavity volume filling), the full volumetric filling stroke of the injection screw during the mold filling process must first be determined. Figure 6 presents the cavity pressure and screw position curves during full volumetric filling. By checking the starting signal at P3 (near the gate) and the volumetrically filled point signal at P8 (at the end of the filling path), the full volumetric filling stroke of the screw can be identified. The full volumetric filling stroke of the screw in the real molding and simulation was 26.94 and 27.20 mm, respectively. The difference was only 0.26 mm (approximately 0.96%), which means that the simulation and real molding were consistent. However, the position of the screws on the front differed (approximately 8 and 16 mm for the real molding and simulation, respectively). Unlike in real molding, rebound movement was not observed immediately after the V/P switchover in the simulation. The pressure on the polymer melt after compression may have differed; this was evaluated in the subsequent experiment.

Having the holding time correspond to the holding pressure is essential for the effect of postfilling (i.e., holding) and determines the geometric accuracy and the inner stress of a part. However, extending the holding time after the gate is frozen is time-consuming and ineffective. The effective holding time can be determined by identifying the point at which the cavity pressure curve becomes unaffected by an increase in holding time. The minimum time is called the "effective holding time." Fig. 7 presents the cavity pressure curves of the near-gate P3 under various holding time settings. The holding time for the real molding and simulation was 5 and 3 s, respectively: a considerable difference (approximately 40%). The real temperature of the polymer melt after it left the nozzle may have differed from that in the simulation, resulting in a difference in heat transfer behavior at the gate. Other differences may

Table 1 Process parameter settings (real molding)

Item	Value				
Melt temperature (°C)	210				
Injection pressure limit (MPa)	240				
Metering position (mm)	52.97				
Suck back stroke (mm)	3				
Injection speed setting:	1st	2nd	3rd	4th	
Screw position (mm)	52.97 → 35	35 → 32.2	32.2 → 12	12 → 6.2	
Injection speed (mm/s)	84	56	70	40	
V/P switchover point (mm)	6.2				
Holding condition setting:	1st	2nd	3rd	4th	5th
Holding pressure (MPa)	110	98	10	30	20
Holding time (s)	0.2	0.25	1.2	1	2.35
Cooling time (s)	20				

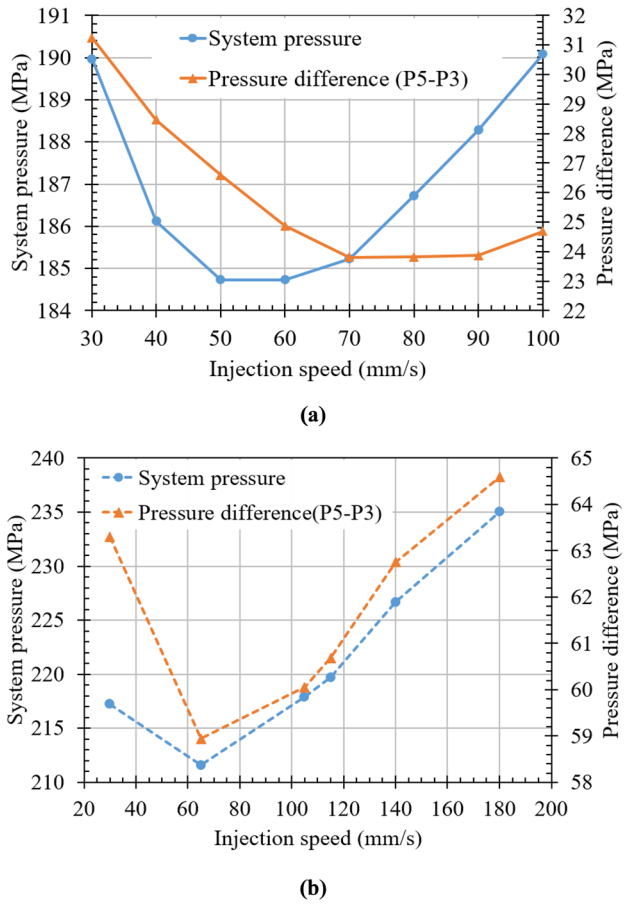

Fig. 5 Pressure drop under different injection speed settings: **a** real molding; **b** simulation

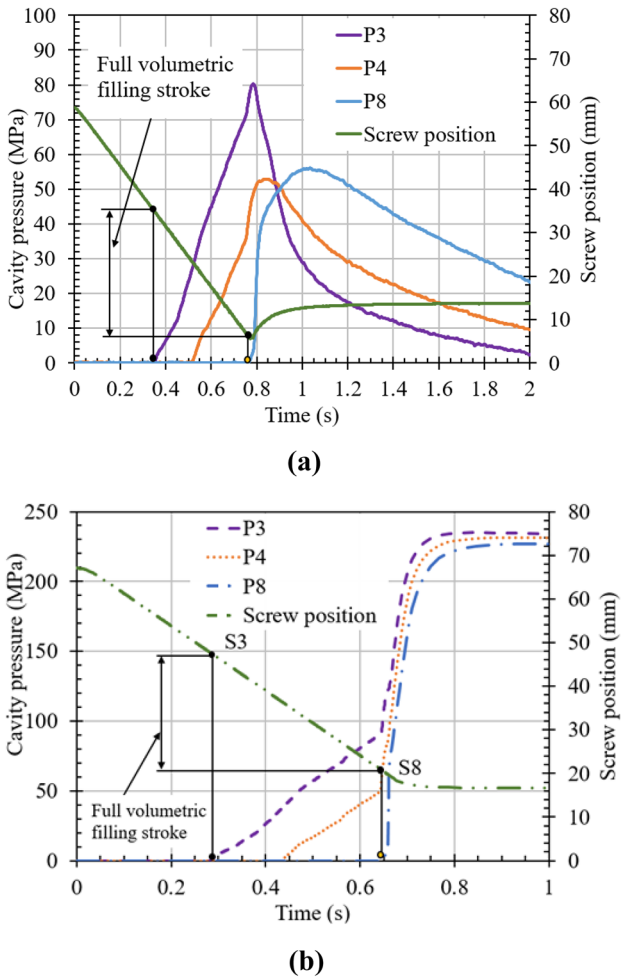

Fig. 6 Cavity pressure and screw position curves during full volumetric filling: **a** real molding; **b** simulation

have been due to the simplified viscoelastic model used to calculate the shear heat dissipation, which should be investigated in future research.

Regarding the optimization of the holding pressure and time during the holding phase, Fig. 8 presents the cavity pressure curves after the multistage holding conditions were set. On the basis of pvT theory, the residual pressures of P3 – P8, representing the position of the polymer melt near the gate, in the middle of the filling path and away from the gate cavity decreased to less than 10 MPa after 7 s, thereby reducing the nonuniform volume at each position before mold opening. This process helped to effectively reduce the change in shrinkage, thereby reducing the warpage of the injection-molded parts. Table 2 presents the widths of the injection-molded parts under single-stage and multistage holding conditions. The volumetric shrinkage rate under the single-stage holding setting was large, which led to considerable warpage of the parts. By contrast, when the multistage holding setting was used, the shrinkage rate decreased to 0.45% (originally 1.18%), thereby controlling the warpage of the part.

5.2 Adjusting the simulation process parameters on the basis of the real system pressure

5.2.1 Before calibration

Figure 9 presents a comparison between the simulated and real system pressure and screw position curves under the same process parameters. The difference in peak system pressure was 47% (real molding: 163 MPa; simulation: 240 MPa). After the V/P switchover point, the system pressure in the simulation reached the maximum (240 MPa), indicating a considerable difference between the simulation and real molding (163 MPa). When the polymer melt entered the cavity from S1 (see Fig. 3), the difference in the melt front position was substantial. Although the simulation and real molding yielded the same screw position curve in the initial filling stage, the difference in the foremost position of the screw was 83% (real molding: 6 mm; simulation: 11 mm). In addition, the simulation failed to predict the

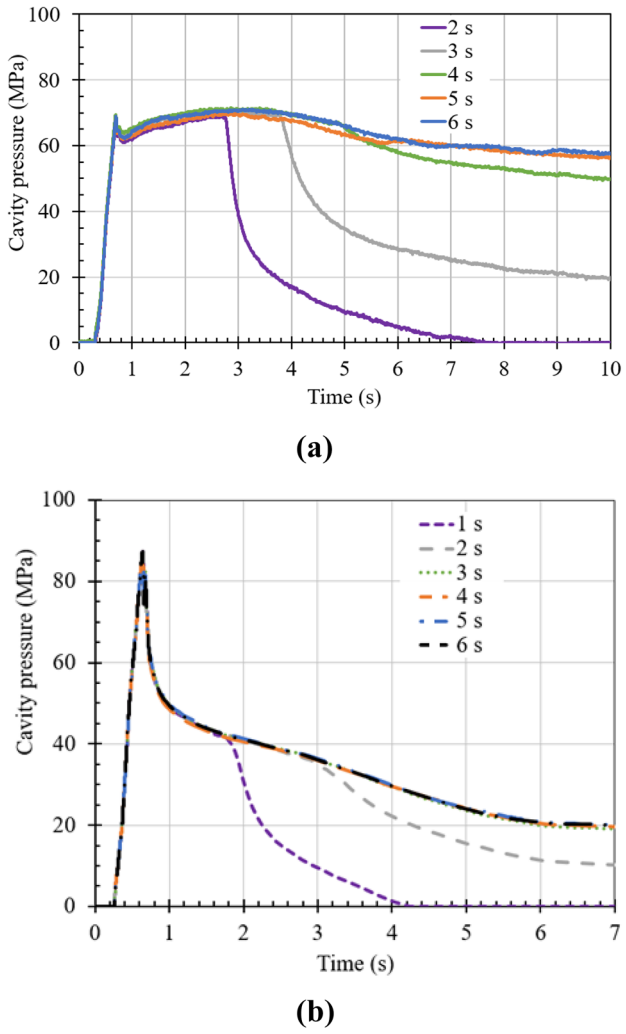

Fig. 7 P3 cavity pressure curves under various holding time settings: **a** real molding; **b** simulation

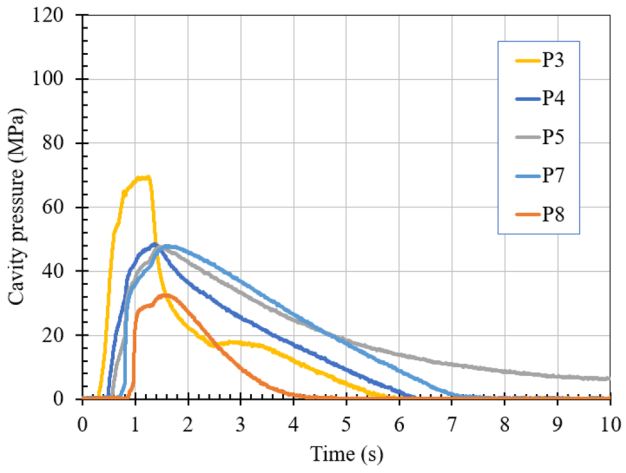

Fig. 8 Cavity pressure curves under multistage holding pressure setting (real molding)

rebound behavior of the injection screw observed in the real molding (1.3 s [Fig. 9]).

5.2.2 Calibrating the full volumetric-filling point with metering adjustment

Because of the inconsistency between the simulation and real molding in terms of the foremost position of the injection screw (difference of 4.67 mm), the metering position of the screw in the simulation was adjusted to 48.3 mm (originally 52.97 mm; Table 1). The real molding and simulation were expected to yield the same foremost position for the injection screw. Figure 10 presents a comparison of the simulated and real system pressure and screw position curves after metering adjustment was performed in the simulation. When the polymer melt entered the cavity from the S1 position, the difference in the position of the melt front decreased. Although a considerable difference in the metering stroke setting (real molding: 52.97 mm; simulation: 44.30 mm) was evident, the foremost position of the screw was consistent, and the rebound behavior of the screw was observed in the simulation. The simulated peak pressure (175 MPa) was similar to that of the real molding (163 MPa).

5.2.3 Calibrating the system pressure curve with injection speed adjustment

To ensure the consistency in the system's peak pressure time between the simulation and real molding, this study adjusted the first-stage injection speed to 70 mm/s (originally 84 mm/s; Table 3). Figure 11 displays the consistency between the simulation and real molding in terms of the system pressure curves. The simulated peak pressure (171 MPa) was similar to that of the real molding (163 MPa). However, the filling time of the full cavity volume in the simulation was lower than that of the real molding, indicating differences in the compression of the polymer melt.

This study examined the various cavity pressure curves in the simulation after the metering and injection speeds were adjusted. Figure 12 presents a comparison of the cavity pressure curves between the simulation and real molding. The P2 and P3 cavity pressure curves were similar between the simulation and real molding (Fig. 12a, b). However, the peak values of P2 and P3 in the simulation were considerably lower than those of the real molding, indicating that the flow resistance at the runner and gate may have been underestimated in the simulation. In the real molding, the peak value of P7 was higher than that in the simulation, indicating an error in the pressure simulation along the filling path. P7 on the slope during the holding and cooling stages was also inaccurate in the simulation. For the P8 cavity pressure curve, the simulation differed substantially from the real molding.

Table 2 Quality comparison between single-stage and multistage holding settings

Condition		W1	W2	W3	W4	W5	Range
Single-stage holding	Width (mm)	59.898	59.800	59.747	29.817	14.798	
	Shrinkage rate (%)	0.16	0.33	0.42	0.60	1.34	1.18
Multi-stage holding	Width (mm)	59.628	59.650	59.673	29.808	14.851	
	Shrinkage rate (%)	0.62	0.58	0.54	0.64	0.99	0.45

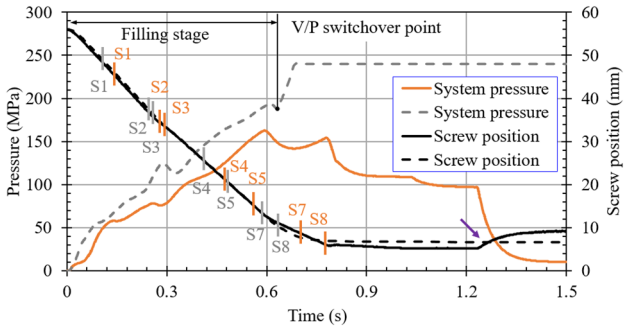

Fig. 9 System pressure and screw position curves (dashed line: simulation; solid line: real molding)

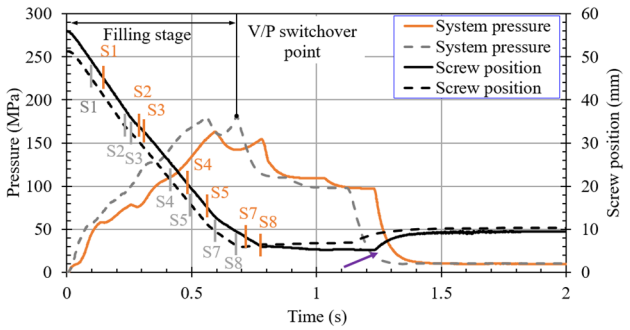

Fig. 10 System pressure and screw position curves (dashed line: simulation after metering adjustment; solid line: real molding)

After the metering stroke and injection speed adjustment, the difference in the metering stroke was 16.3% (real molding: 52.97 mm; simulation: 44.3 mm). The difference in the foremost position of the screw was 0.8% (real molding: 6.18 mm; simulation: 6.13 mm). The difference in the system's peak pressure was 4.9% (real molding: 163 MPa; simulation: 171 MPa). The difference in peak P3 pressure was 1.4% (real molding: 70 MPa; simulation: 71 MPa). The difference in peak P8 pressure was 93.8% (real molding: 32 MPa; simulation: 2 MPa).

5.2.4 Calibrating the cavity pressure curve with V/P switchover point adjustment

To ensure the simulated P8 cavity pressure curves were consistent, this study adjusted the V/P switchover point to 5.4 mm (originally 6.2 mm). The real peak system pressure was lower than that in the simulation, and the foremost positions of the screw were inconsistent. The P1 and P2 cavity pressure curves were similar between the simulation and real molding. However, the peak values of P1 (Fig. 13a) and P2 (Fig. 13b) in the simulation differed from those in the real molding, suggesting that the flow resistance at the runner and gate may have been underestimated in the simulation. In the real molding, the peak value for P3 (Fig. 13c) was lower than that in the simulation, indicating an error in the pressure simulation along the filling path. The

Table 3 Process parameter settings in the simulation (adjusted metering and injection speed)

Item	Value				
Melt temperature (°C)	210				
Injection pressure limit (MPa)	240				
Metering position (mm)	44.30				
Suck back stroke (mm)	3				
Injection speed setting:	1st	2nd	3rd	4th	
Screw position (mm)	44.3 → 35	35 → 32.2	32.2 → 12	12 → 6.2	
Injection speed (mm/s)	70	56	70	40	
V/P switchover point (mm)	6.2				
Holding condition setting:	1st	2nd	3rd	4th	5th
Holding pressure (MPa)	110	98	10	30	20
Holding time (s)	0.2	0.25	1.2	1	2.35
Cooling time (s)	20				

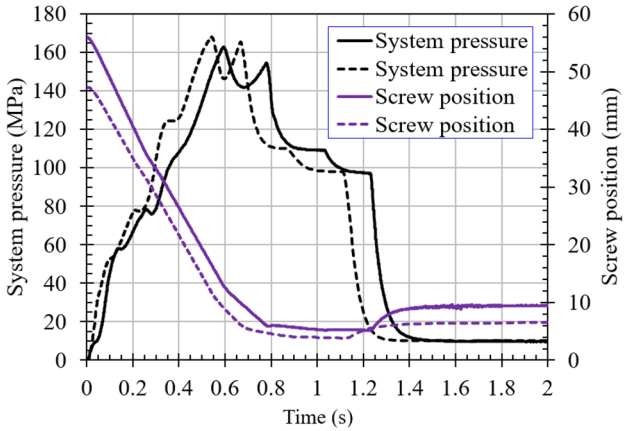

Fig. 11 System pressure and screw position curves (dash line: simulation after metering and injection speed adjustment; solid line: solid line)

simulation of P3 on the slope during the holding and cooling stages was accurate. In terms of the P8 cavity pressure curve (Fig. 13d), the simulation was highly consistent with the real molding.

After adjustment to the metering stroke, injection speed, and V/P switchover point, the difference in metering stroke was 16.3% (real molding: 52.97 mm; simulation: 44.3 mm). The difference in the foremost position of the screw was 13.3% (real molding: 6.18 mm; simulation: 5.36 mm). The difference in peak system pressure was 4.9% (real molding: 163 MPa; simulation: 171 MPa). The difference in peak P3 pressure was 5.7% (real molding: 70 MPa; simulation: 74 MPa). The difference in peak P8 pressure was 6.3% (real molding: 32 MPa; simulation: 30 MPa).

5.3 Width quality

Table 4 lists the width quality of the injection-molded part predicted by the simulation and that observed in the real molding. Figure 14 presents a comparison of their width shrinkage rates.

1. Under identical process parameter settings, the system pressure in the simulation was higher than that of the real molding, resulting in a larger width in the simulation. The negative value for the shrinkage rate in the simulation indicated an increase in width caused by overpacking.
2. After adjustment to the metering stroke and injection speed, the consistency between the simulated and real molding system pressures led to similar width quality.
3. After adjustment to the V/P switchover point, the consistency between the simulated and real molding cavity pressure was expected to produce similar width

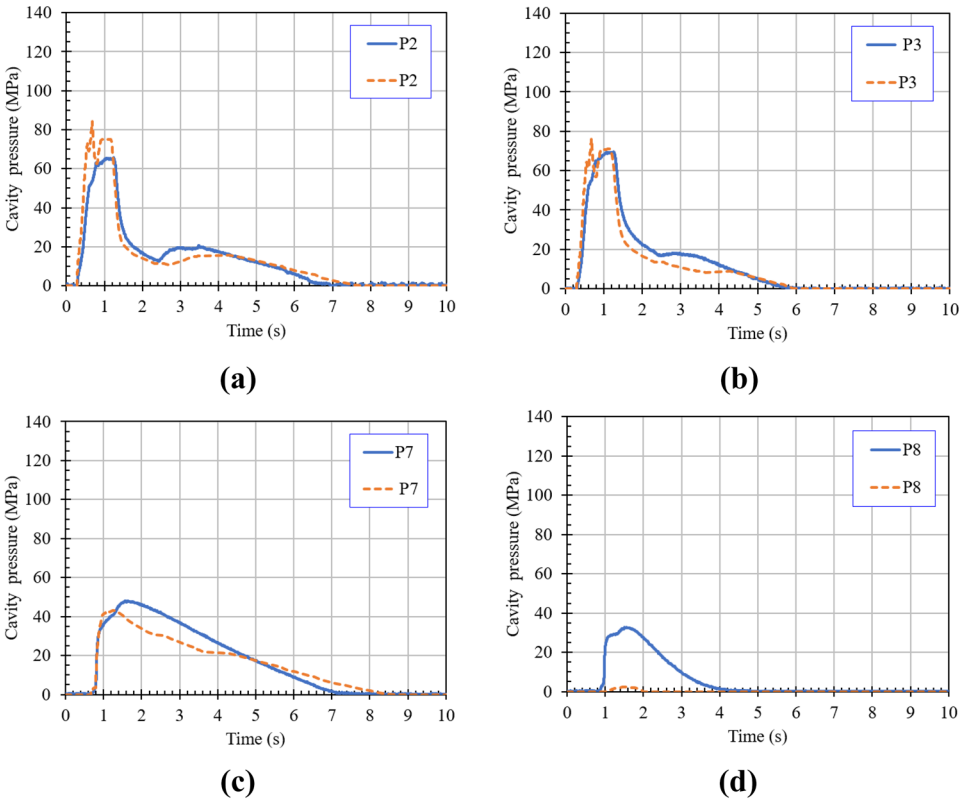

Fig. 12 Cavity pressure curves (dash line: simulation after metering and injection speed adjustment; solid line: real molding)

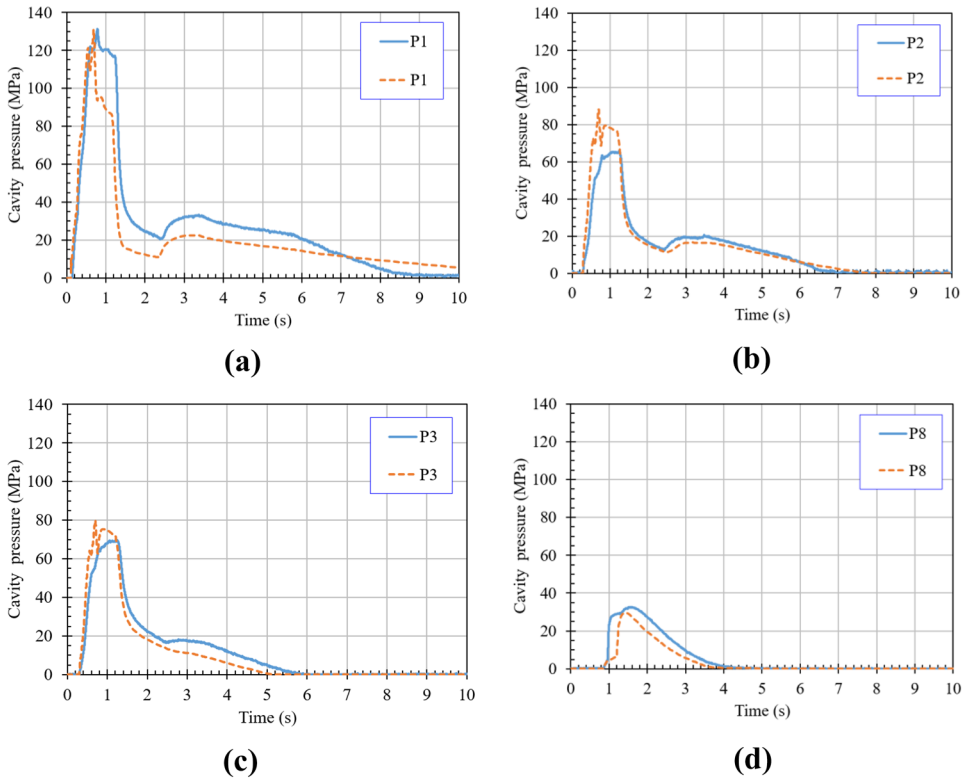

Fig. 13 Cavity pressure curves (dash line: simulation after V/P switchover point adjustment; solid line: real molding)

Table 4 Width quality

Condition		W1	W2	W3	W4	W5	Range
Real molding	Width (mm)	59.628	59.650	59.673	29.808	14.851	
	Shrinkage (%)	0.62	0.58	0.54	0.64	0.99	0.45
Simulation	Width (mm)	61.209	61.132	61.111	30.52	15.281	
	Shrinkage (%)	−2.02	−1.89	−1.85	−1.76	−1.87	0.29
Simulation with metering stroke adjustment	Width (mm)	59.963	60.085	60.164	30.074	15.109	
	Shrinkage (%)	0.06	−0.14	−0.27	−0.25	−0.73	0.79
Simulation with metering stroke, injection speed adjustment	Width (mm)	59.884	59.917	59.949	29.951	14.965	
	Shrinkage (%)	0.19	0.14	0.09	0.16	0.23	0.14
Simulation with metering stroke, injection speed, V/P adjustment	Width (mm)	59.899	59.951	59.990	29.974	14.990	
	Shrinkage (%)	0.16	0.08	0.01	0.16	0.06	0.15

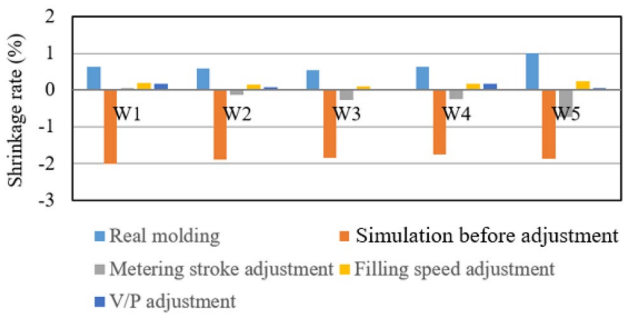

Fig. 14 Comparison of width shrinkage rate between real molding and simulation with adjusted parameters

quality. However, the real cavity pressure was lower than the simulated value, resulting in a high shrinkage rate. Adjusting the V/P switchover point can affect the holding conditions in the simulation and result in a low shrinkage rate. The improvements in W3 and W5 were notable. The geometrical locations of W1 and W4 may have prevented the transfer of holding pressure, resulting in ineffective packing.

6 Conclusion

The accuracy of mold flow simulation is essential to intelligent injection mold manufacturing. However, simulation technology is limited by several factors, resulting in inconsistencies when compared with real molding. This study applied in-mold machine sensing information to determine the optimal process parameter settings for real molding and then adjusted the process parameters in the simulation on the basis of the real pressure and screw position curves, thereby decreasing the difference between the simulated and real pressure curves. The results are as follows:

1. Before the process parameter adjustment, the difference in the foremost position of the screw was 83% (real molding: 6 mm; simulation: 11 mm). The difference in peak system pressure was 47% (real molding: 163 MPa; simulation: 240 MPa). The system pressure in the simulation was considerably higher than that in the real molding, resulting in a larger simulated width. The negative value for the shrinkage rate in the simulation indicated an increase in width caused by overpacking.
2. After adjusting the metering stroke and injection speed, the difference in the metering stroke decreased to 16.3% (real molding: 52.97 mm; simulation: 44.3 mm). The difference in the foremost position of the screw was only 0.8% (real molding: 6.18 mm; simulation: 6.13 mm). The difference in peak system pressure decreased to 4.9% (real molding: 163 MPa; simulation: 171 MPa). The difference in peak P3 pressure was only 1.4% (real molding: 70 MPa; simulation: 71 MPa). However, the difference in peak P8 pressure was 93.8% (real molding: 32 MPa; simulation: 2 MPa). Overall, except for the far-from-gate cavity pressure curves, the consistency between the simulation and real molding system pressure led to similar width quality.
3. After adjusting the V/P switchover point, the difference in peak P8 pressure decreased considerably to 6.3% (real molding: 32 MPa; simulation: 30 MPa). The differences in metering stroke, foremost position of the screw, peak system pressure, and peak P3 pressure increased to 16.3%, 13.3%, 4.9%, and 5.7%, respectively. The real cavity pressure was lower than the simulated value, resulting in a high shrinkage rate. Adjusting the V/P switchover point can affect the holding conditions in the simulation and result in a low shrinkage rate. The improvements in W3 and W5 were notable. The geometrical locations of W1 and W4 may have prevented the transfer of holding pressure, resulting in ineffective packing.
4. This study demonstrated the potential of the proposed method to enable reduction of the difference between the simulated and real pressure and screw position curves through adjustment of the process parameter settings during a simulation. Subsequent studies should develop a fast and systematic method to identify the optimal process parameter settings during the simulation of various injection molding applications.

Author contribution S.-C. Nian and M.-S. Huang were responsible for deriving conceptualization and methodology. B.-W. Wang was responsible for simulation and experiment. B.-W. Wang and M.-S. Huang were involved in the discussion and significantly contributed to making the final draft of the article. All the authors read and approved the final manuscript.

Data availability The authors confirm that the data supporting the findings of this study are available within the article.

Declarations

Ethics approval Not applicable.

Consent to participate Not applicable.

Consent for publication Not applicable.

Competing interests The authors declare no competing interests.

References

1. Fassett K (2009) Scientific molding, in-cavity sensors, and data management. RJG Inc
2. Chen JY, Yang KJ, Huang MS (2018) Online quality monitoring of molten resin in injection molding. Int J Heat Mass Transf 122:681–693
3. Wang J, Mao Q (2013) A novel process control methodology based on the PVT behavior of polymer for injection molding. Adv Polym Technol 32(S1):474–485
4. Zhang N, Gilchrist MD (2012) Characterization of thermos-rheological behavior of polymer melts during the micro injection molding process. Polym Test 31:748–758
5. ENGEL (2019) Self-adjusting assistance systems for machines and robots. ENGEL Tech Rep
6. Kurt M, Saban KO, Kaynak Y, Atakok G, Girit O (2009) Experimental investigation of plastic injection molding: assessment of the effects of cavity pressure and mold temperature on the quality of the final products. Mater Des 30:3217–3224
7. Wang J, Xie P, Ding Y, Yang W (2009) On-line testing equipment of P-V-T properties of polymers based on an injection molding machine. Polym Test 28(3):228–234
8. Lin CC, Wang WT, Kuo CC, Wuet CL (2014) Experimental and theoretical study of melt viscosity in injection process. Int J Mech Mechatronics Eng 8(7):687–691
9. Gornik C (2008) Viscosity measuring methods for feedstocks directly on injection molding machines. Mater Sci Forum 591–593:174–178
10. Chen JY, Tseng CC (2019) Huang MS (2019) Quality indexes design for online monitoring polymer injection molding. Adv Polym Technol 419:1–20

11. Zhou X, Zhang Y, Mao T, Zhou H (2017) Monitoring and dynamic control of quality stability for injection molding process. J Mater Process Technol 249:385–366
12. Aho J, Syrjälä S (2011) Shear viscosity measurements of polymer melts using injection molding machine with adjustable slit die. Polym Test 30:595–601
13. Huang MS, Nian SC, Chen JY, Lin CY (2018) Influence of clamping force on tie-bar elongation, mold separation, and part dimensions in injection molding. Precis Eng 51:647–658
14. Huang MS, Lin CY (2017) A novel clamping force searching method based on sensing tie-bar elongation for injection molding. Int J Heat Mass Transf 109:223–1230
15. Chen JY, Yang KJ, Huang MS (2020) Optimization of clamping force for low-viscosity polymer injection molding. Polym Test 90:106700
16. Zhang JF, Zhao P, Zhao Y, Xia N, Fu JZ (2019) On-line measurement of cavity pressure during injection molding via ultrasonic investigation of tie bar. Sens Actuator A-Phys 285:118–126
17. Zhao P, Zhou H, He Y, Cai K, Fu J (2014) A nondestructive online method for monitoring the injection molding process by collecting and analyzing machine running data. Int J Adv Manuf Technol 72:765–777
18. Kazmer DO, Velusamy S, Westerdale S, Johnston S, Gao RX (2010) A comparison of seven filling to packing switchover methods for injection molding. Polym Eng Sci 50:2031–2043
19. Kazmer D, Barkan P (1997) Multi-cavity pressure control in the filling and packing stages of the injection molding process. Polym Eng Sci 37:1865–1879
20. Gim J, Rhee B (2021) Novel analysis methodology of cavity pressure profiles in injection-molding processes using interpretation of machine learning model. Polymers 13:3297
21. Beaumont J (2012) Brand-new test method relates material, mold & machine. Plastics Technol
22. Hopmann Ch, Zhuang J (2017) Process control strategies for injection molding processes with changing raw material viscosity. J Polym Eng 38(5):483–492
23. Kulkarni S (2015) Scientific molding the six step study. https://www.fimmtech.com
24. Karbasi H (2006) Smart mold: real time in cavity data acquisition. First annual technical showcase & third annual workshop, Citeseer, Canada
25. Nian SC, Fang YC, Huang MS (2019) In-mold and machine sensing and feature extraction for optimized IC-tray manufacturing. Polymers 11(8):1348–1366
26. Chang YH, Wei TH, Chen SC, Lou YF (2020) The investigation on PVT control method establishment for scientific injection molding parameter setting and its quality control. Polym Eng Sci 60:2895–2907
27. Guerrier P, Tosello G, Hattel JH (2017) Flow visualization and simulation of the filling process during injection molding. CIRP J Manuf Sci Technol 16:220–222
28. Regi F, Guerrier P, Zhang Y, Tosello G (2020) Experimental characterization and simulation of thermoplastic polymer flow hesitation in thin-wall injection molding using direct in-mold visualization technique. Micromachines 11(4):428–440
29. Huang CT, Hsu YH, Chen BS (2018) Investigation on the internal mechanism of the deviation between numerical simulation and experiments in injection molding product development. Polym Test 75:327–336
30. Huang CT, Xu RT, Chen PH, Jong WR, Chen SC (2020) Investigation on the machine calibration effect on the optimization through design of experiments (DOE) in injection molding parts. Polym Test 90:106703
31. Huang MS, Liu CY, Ke KC (2021) Calibration of cavity pressure simulation using autoencoder and multilayer perceptron neural networks. Polym Eng Sci 61:2511–2521
32. Chen JY, Hung PH, Huang MS (2021) Determination of process parameters based on cavity pressure characteristics to enhance quality uniformity in injection molding. Int J Heat Mass Transf 180:121788
33. Coretech System Co Ltd (2019) Computer-implemented simulation method for injection-molding process. US Patent 16:587858